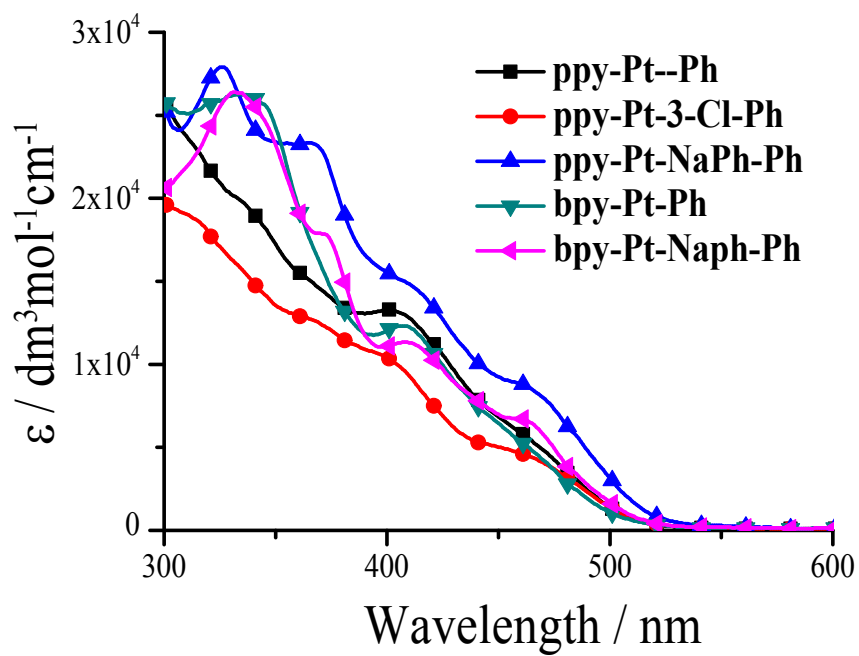


## **Supporting Information**

# **Syntheses, crystal structures, chirality and aggregation-induced phosphorescence of stacked binuclear platinum(II) complexes with bridging Salen ligands**

**Lang Qu, Li Chunbo, Guangyu Shen, Fei Gou, Jintong Song, Man Wang, Xuemei Xu,  
Xiangge Zhou, and Haifeng Xiang\***

**College of Chemistry, Sichuan University, Chengdu, 610041, China**



**Fig. S1.** Absorption spectra of Pt(II) complexes with  $\mu$ -Ph bridges in THF.

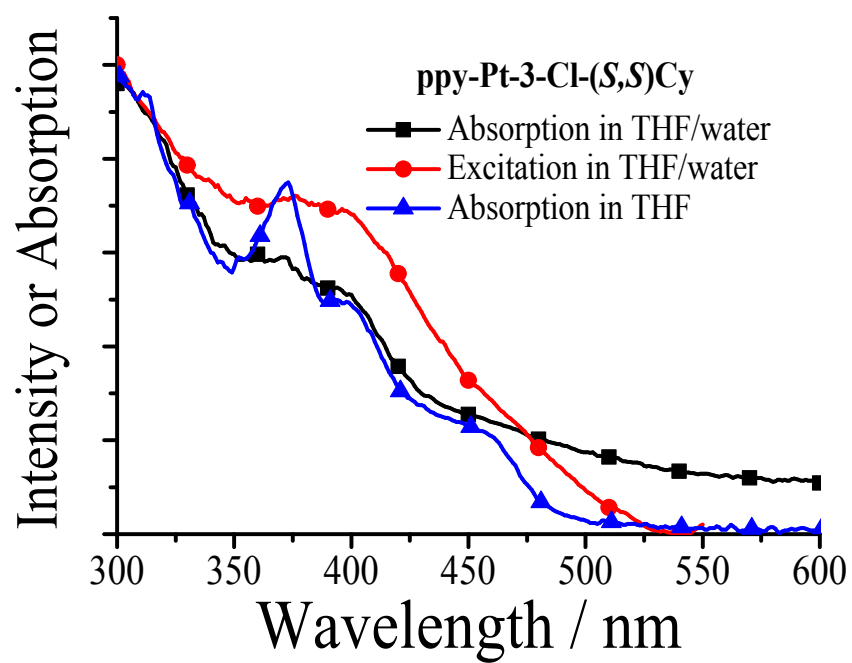
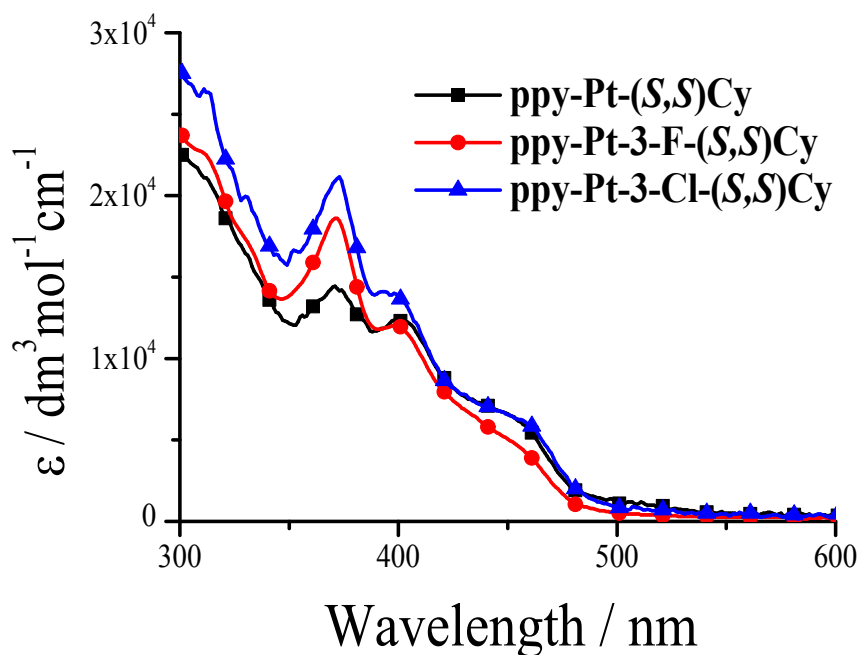


**Fig. S2.** Top: Absorption spectra of Pt(II) complexes with  $\mu$ -(*S,S*)Cy bridges in THF. Bottom: Absorption and excitation spectra of ppy-Pt-3-Cl-(*S,S*)Cy ( $2.0 \times 10^{-5} \text{ mol dm}^{-3}$ ) in THF and THF/water (water 96%).

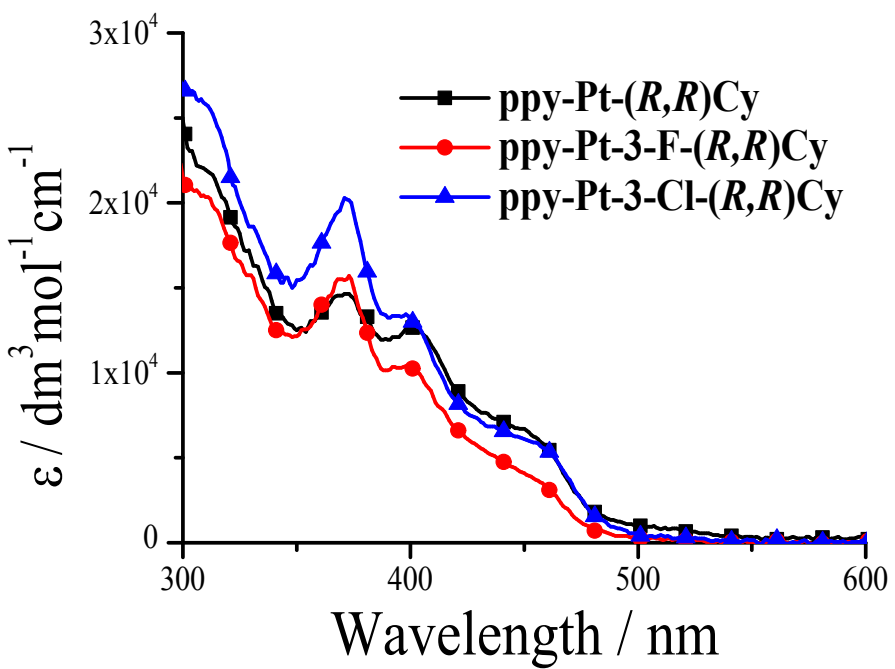


**Fig. S3.** Absorption spectra of Pt(II) complexes with  $\mu$ -(*R,R*)Cy bridges in THF.

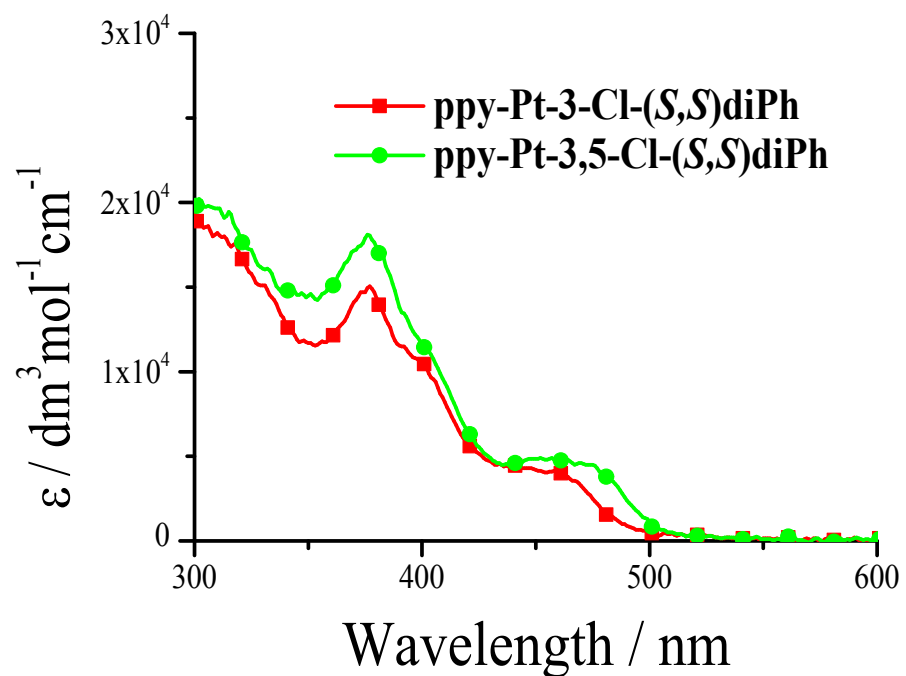


**Fig. S4.** Absorption spectra of Pt(II) complexes with  $\mu$ -(*S,S*)diPh bridges in THF.

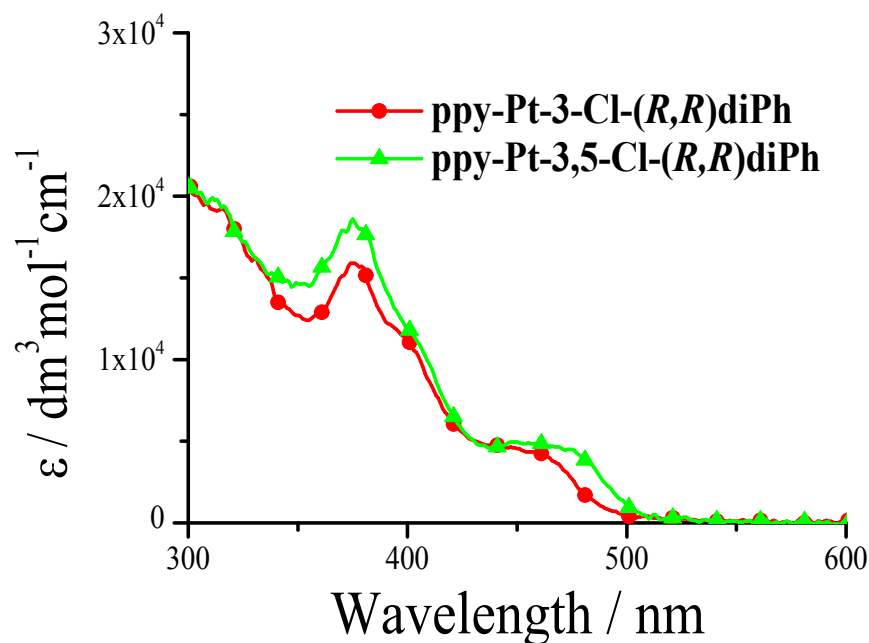


**Fig. S5.** Absorption spectra of Pt(II) complexes with  $\mu$ -(*R,R*)diPh bridges in THF.

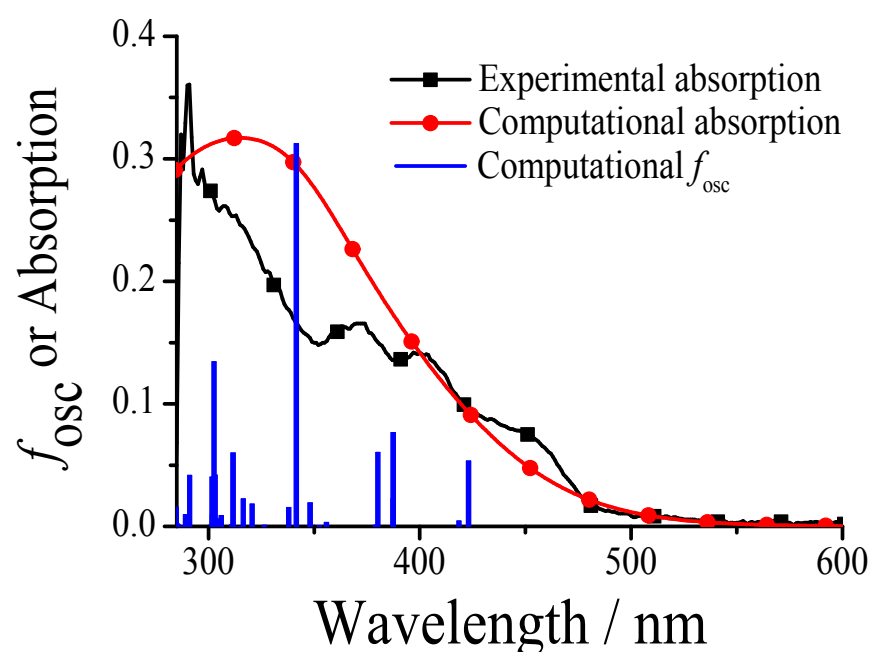


**Fig. S6.** Computational and experimental (in THF) absorption spectra of ppy-Pt-(*S,S*)Cy.

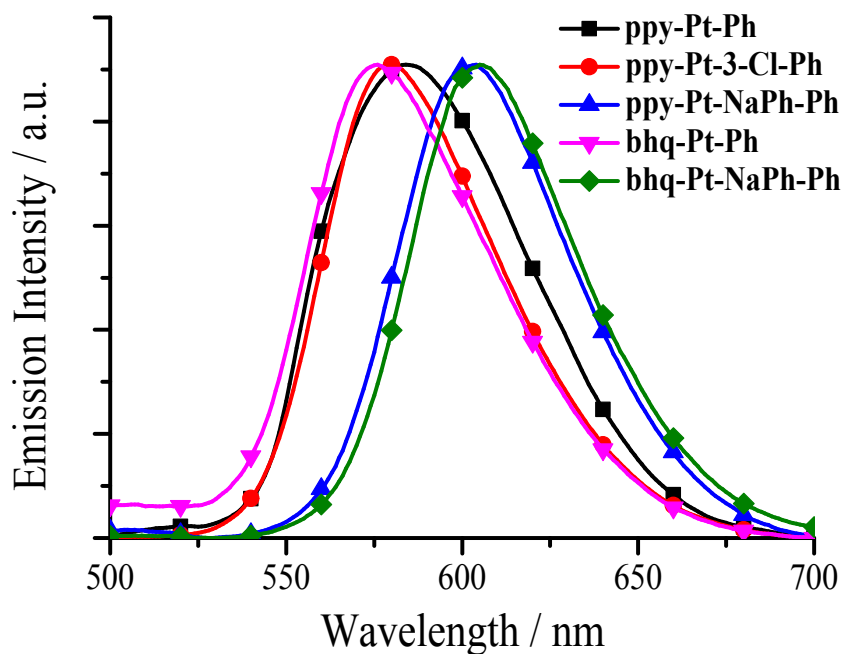


**Fig. S7.** Normalized emission spectra of Pt(II) complexes with  $\mu$ -Ph bridges in solid.

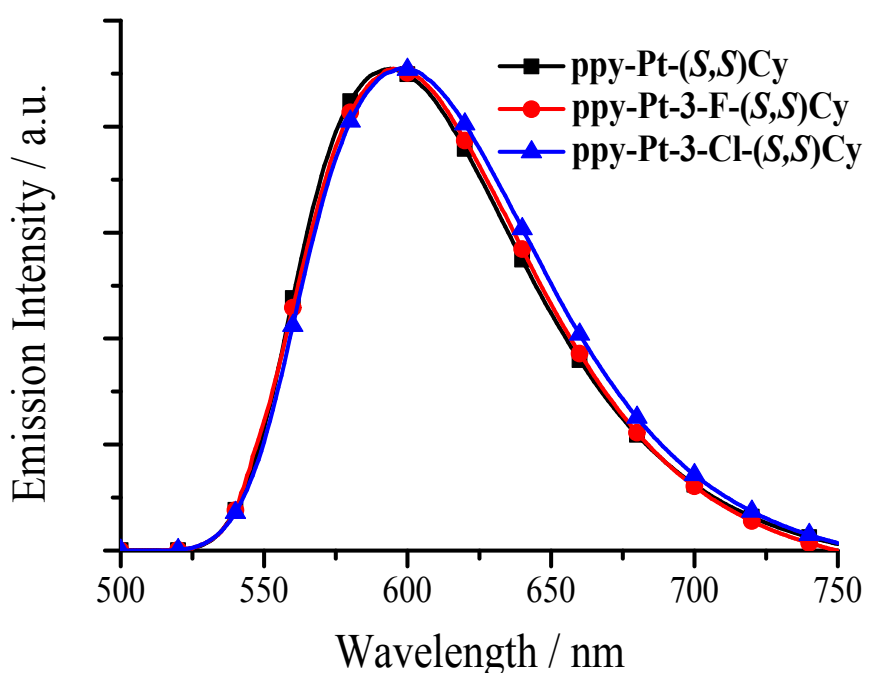


**Fig. S8.** Normalized emission spectra of Pt(II) complexes with  $\mu$ -(*S,S*)Cy bridges in solid.

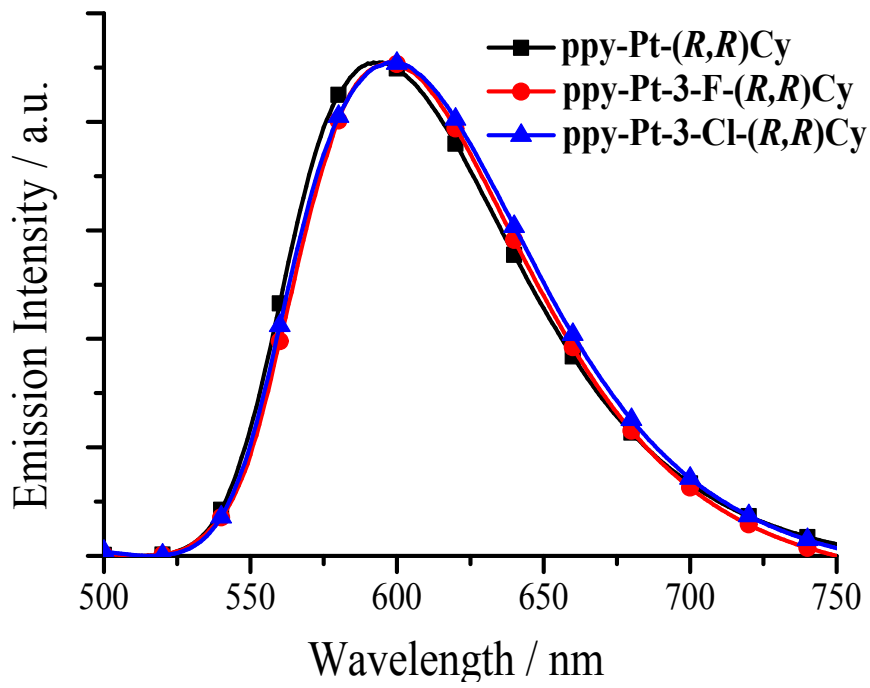


**Fig. S9.** Normalized emission spectra of Pt(II) complexes with  $\mu$ -(*R,R*)Cy bridges in solid.

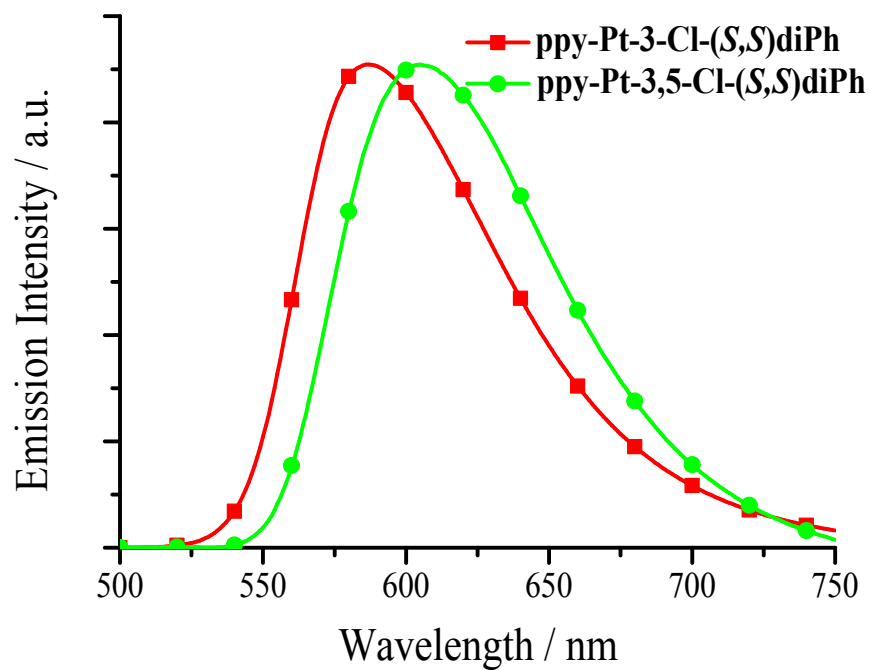


**Fig. S10.** Normalized emission spectra of Pt(II) complexes with  $\mu$ -(*S,S*)diPh bridges in solid.

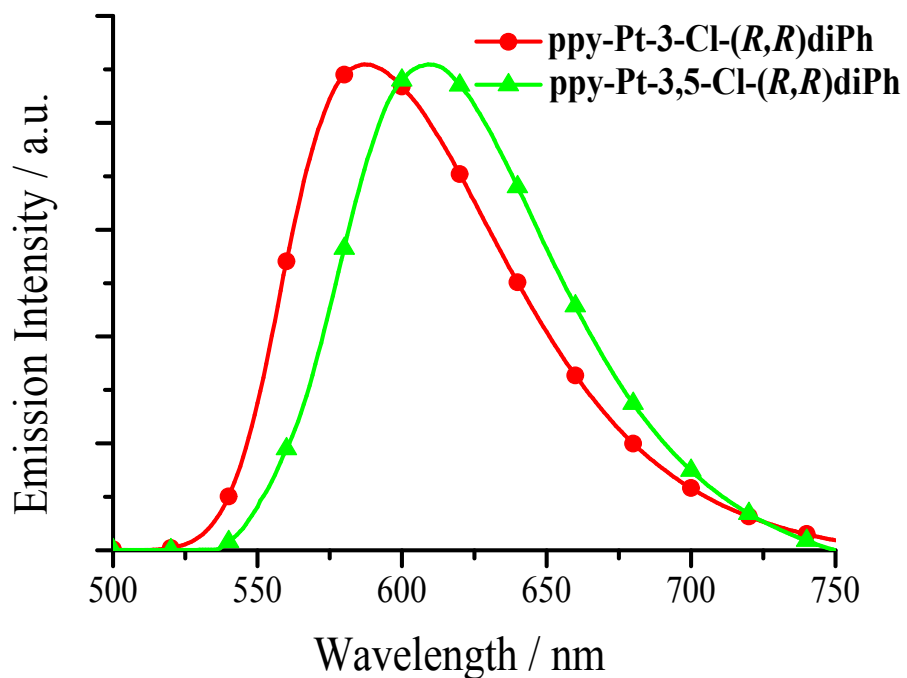


**Fig. S11.** Normalized emission spectra of Pt(II) complexes with  $\mu$ -(*R,R*)diPh bridges in solid.

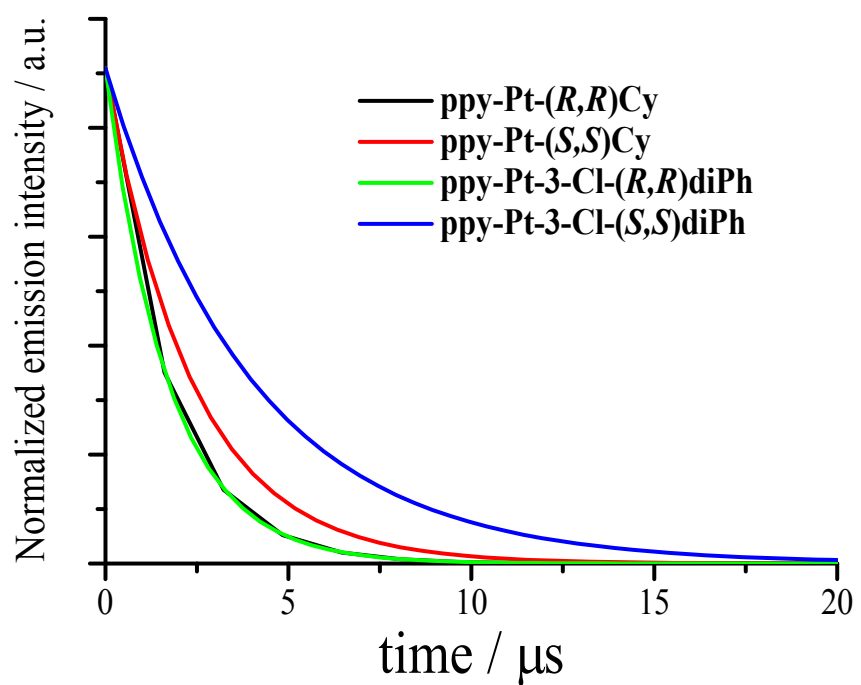


**Fig. S12.** Normalized emission decay spectra of Pt(II) complexes (excited at 400 nm).

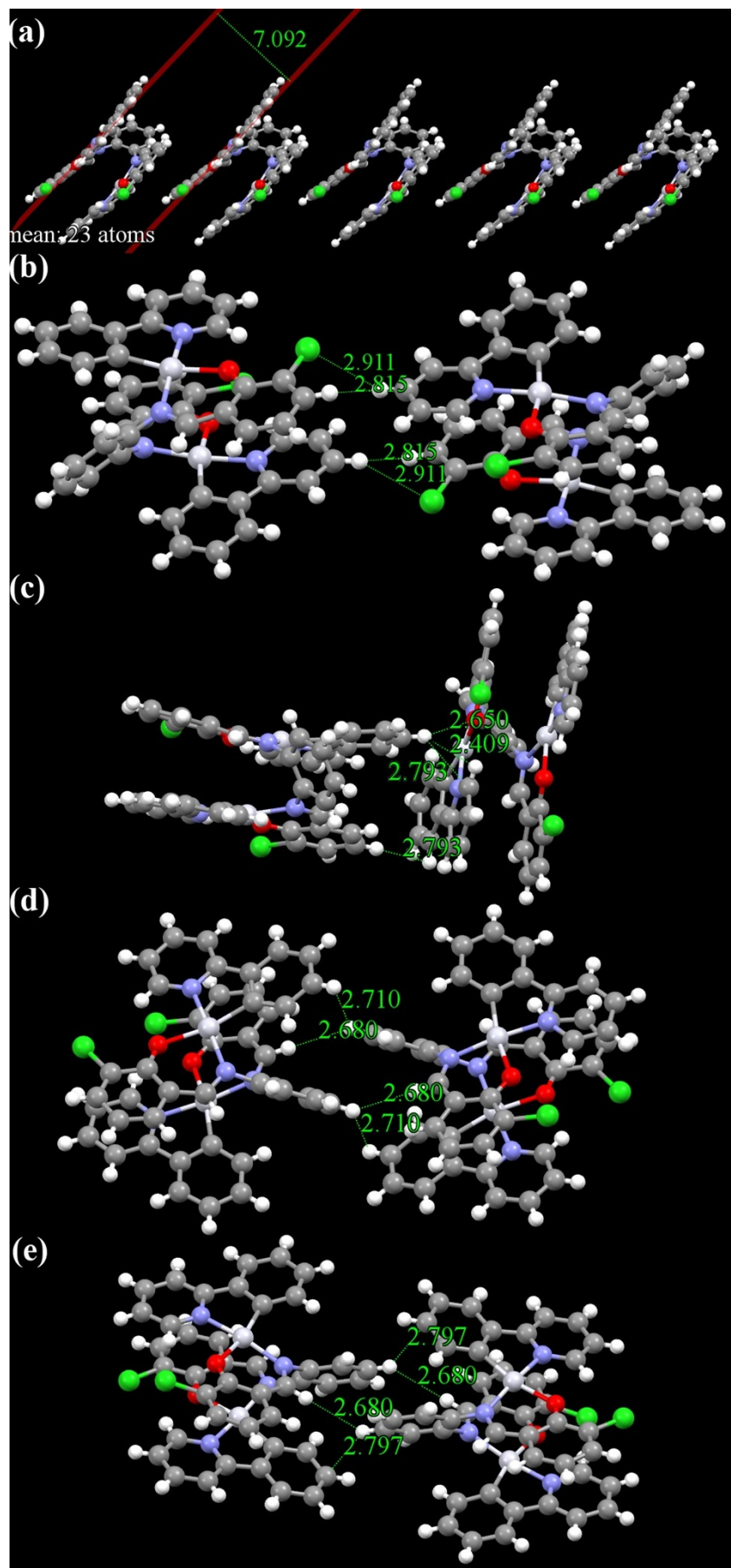


**Fig. S13.** X-ray single crystal structures and packings of **ppy-Pt-3-Cl-Ph** molecules (intermolecular interactions of the two neighboring molecules).

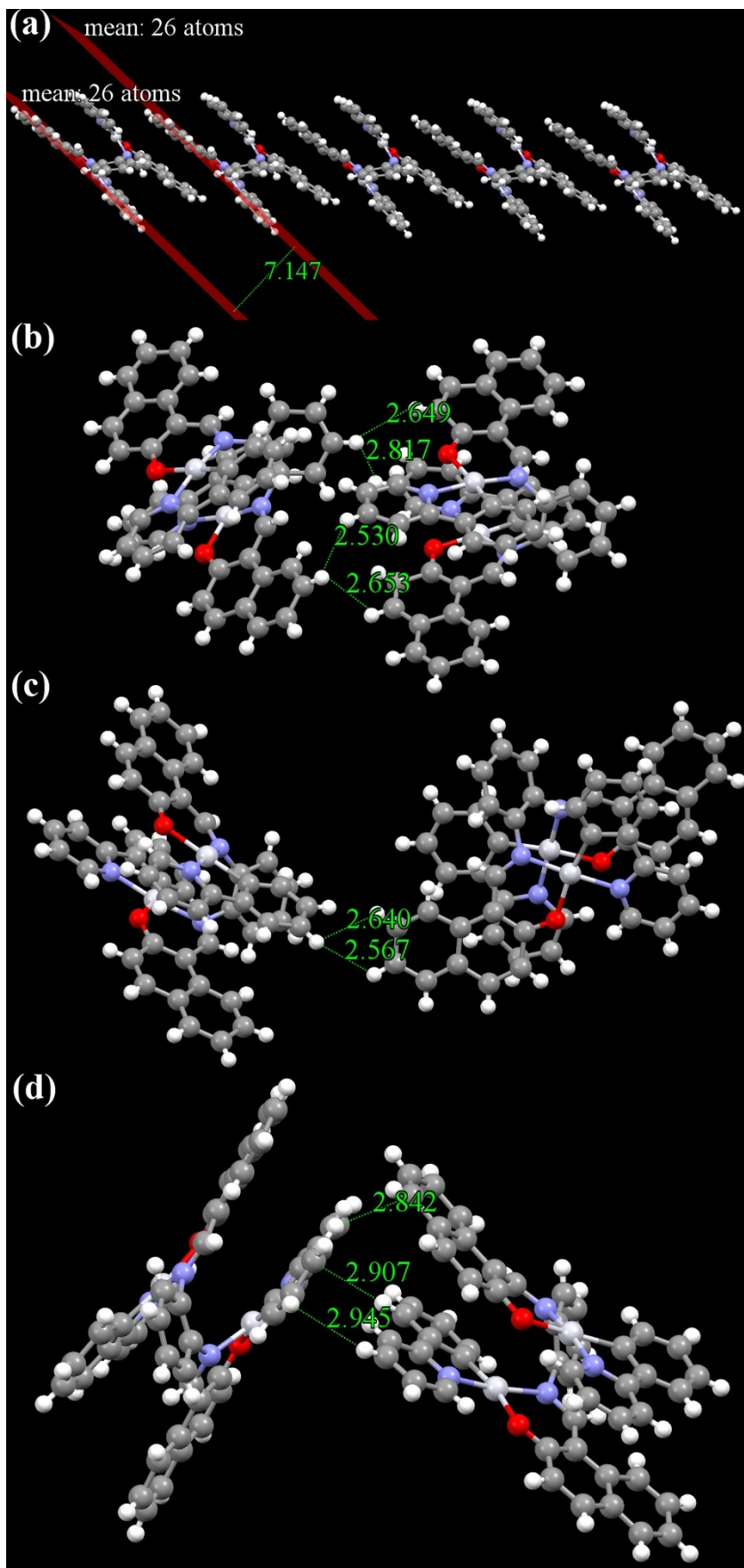


**Fig. S14.** X-ray single crystal structures and packings of **ppy-Pt-Naph-Ph** molecules (intermolecular interactions of the two neighboring molecules). CHCl<sub>3</sub> solvent molecules are omitted.

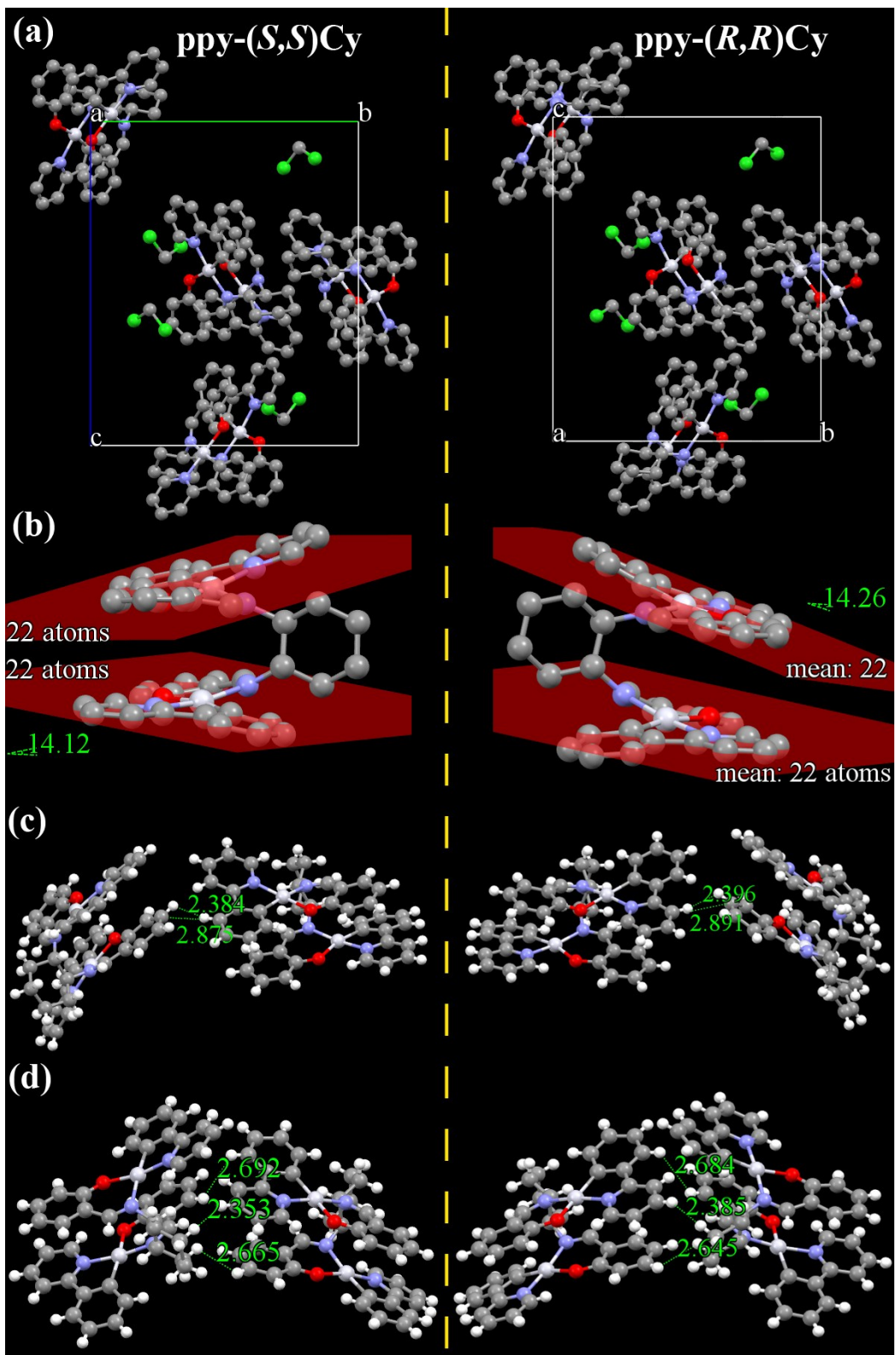


**Fig. S15.** X-ray single crystal structures and packings of ppy-Pt-(*S,S*)Cy and ppy-Pt-(*R,R*)Cy molecules (intermolecular interactions of the two neighboring molecules). Some H atoms and CH<sub>2</sub>Cl<sub>2</sub> solvent molecules are omitted.

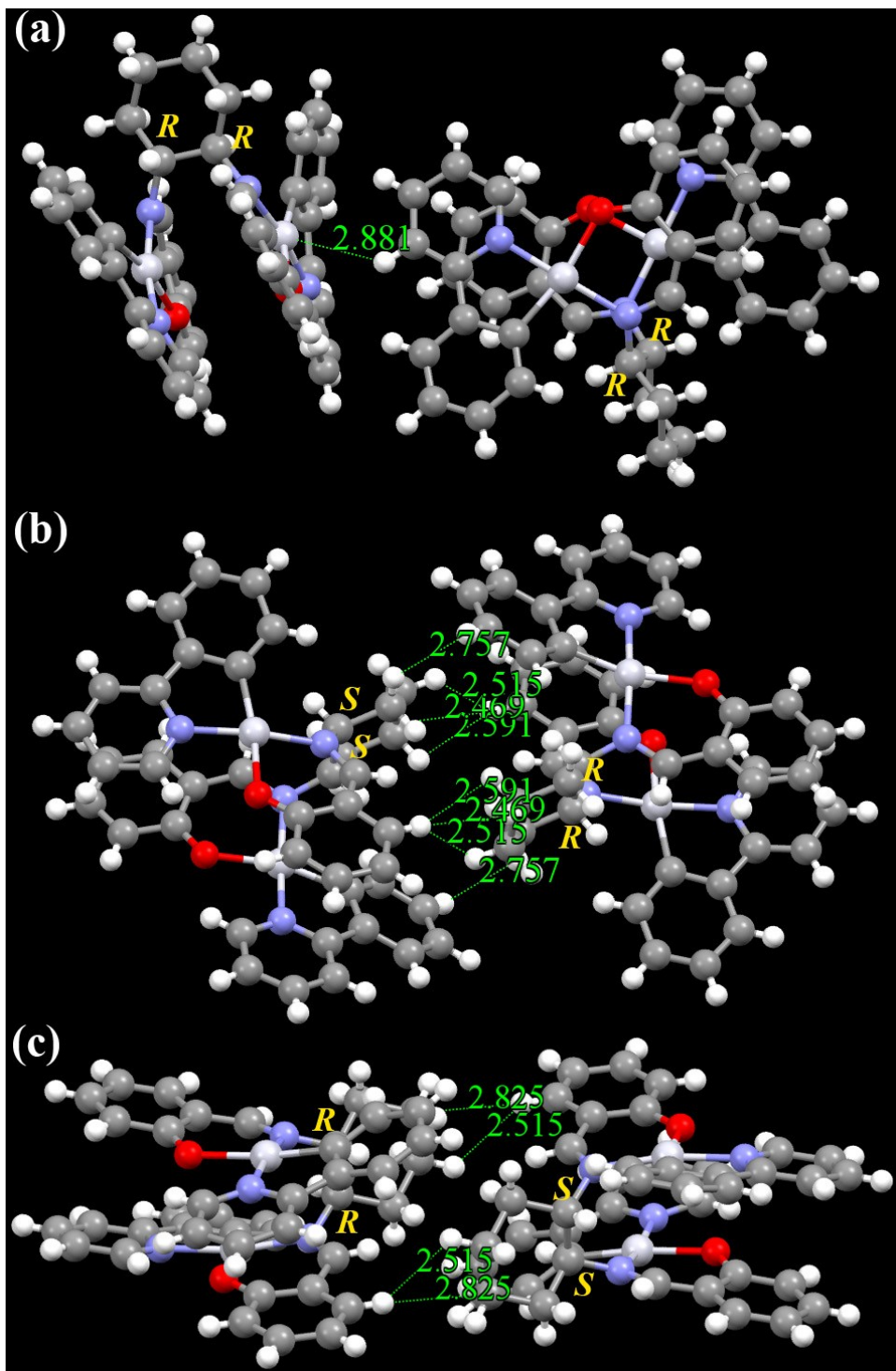


**Fig. S16.** Intermolecular interactions of two neighboring molecules in X-ray single crystals of racemic **ppy-Pt-Cy**.

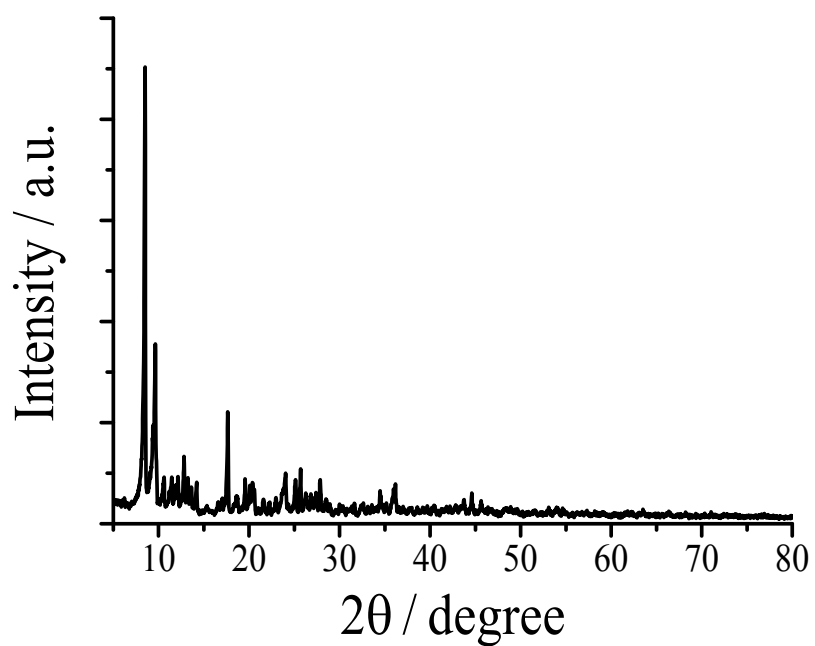


**Fig. S17.** X-ray powder diffraction spectra of **ppy-Pt-3-F-(S,S)Cy** solid.

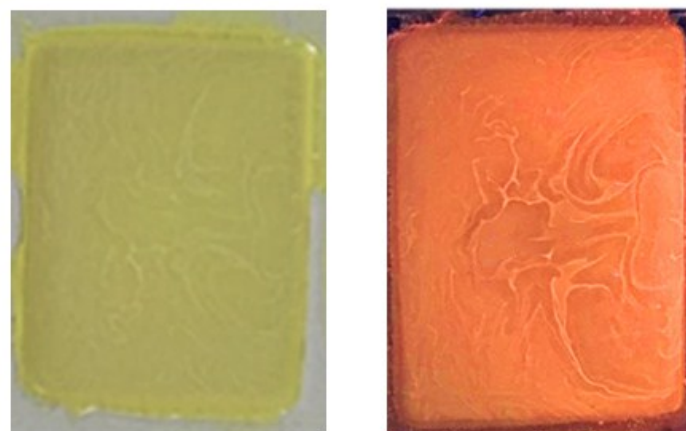


**Fig. S18.** Casting film of **ppy-Pt-3-F-(S,S)Cy**-doped PMMA (5.0 wt%) under room light (left) and 360 nm UV light (right).

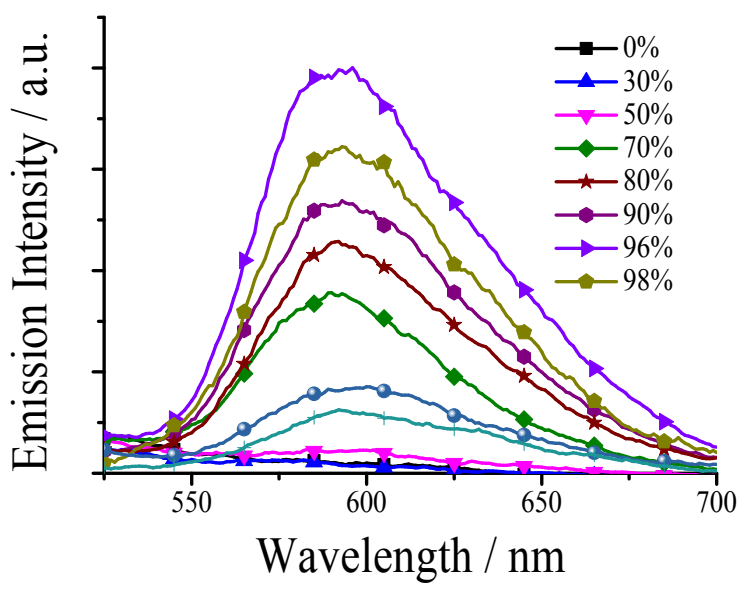
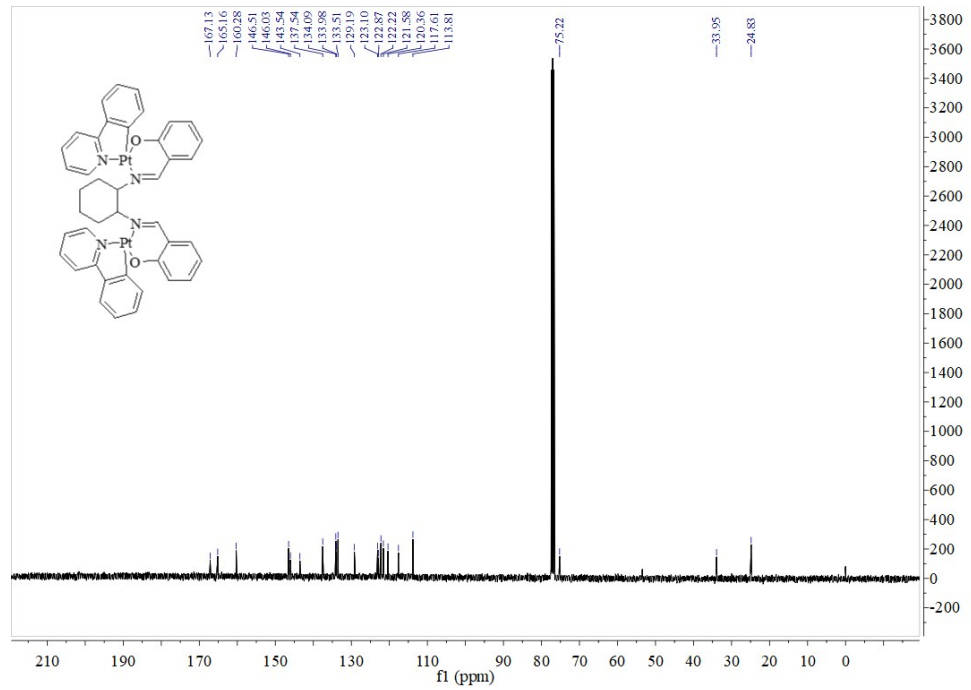
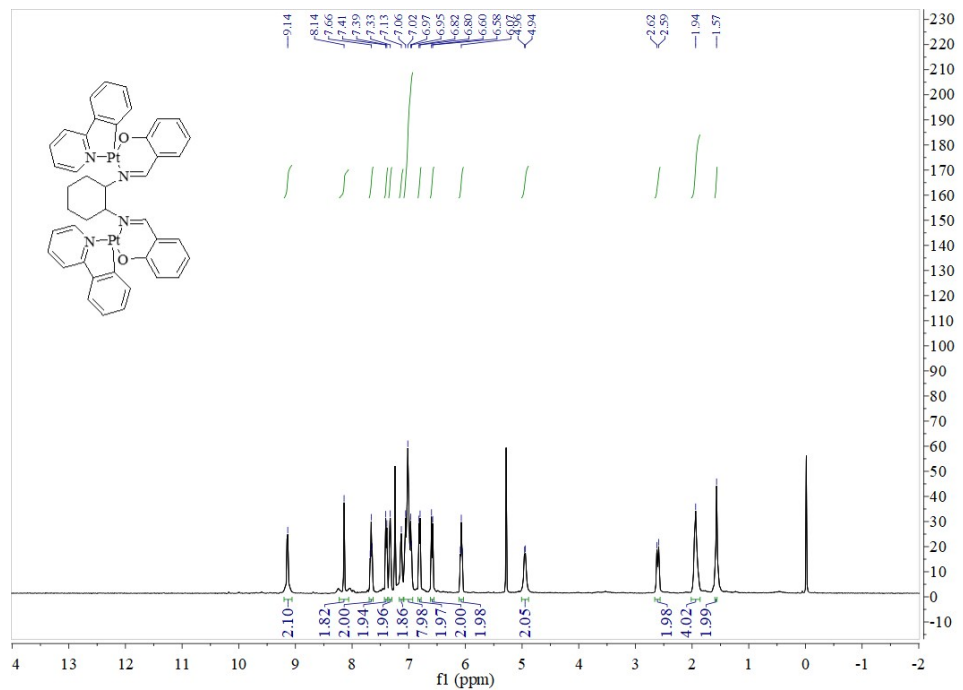
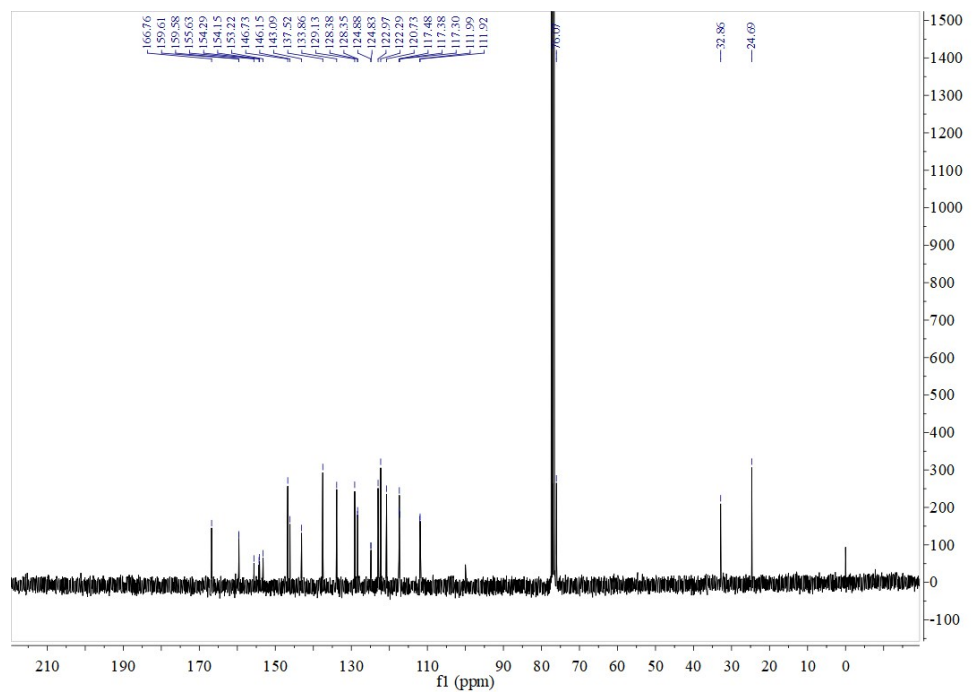
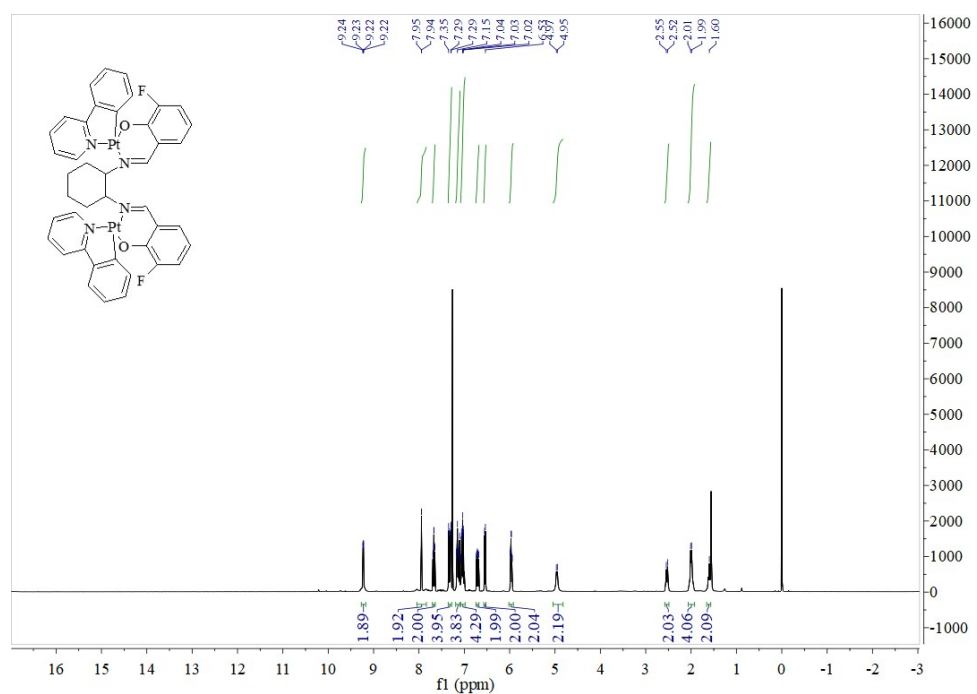


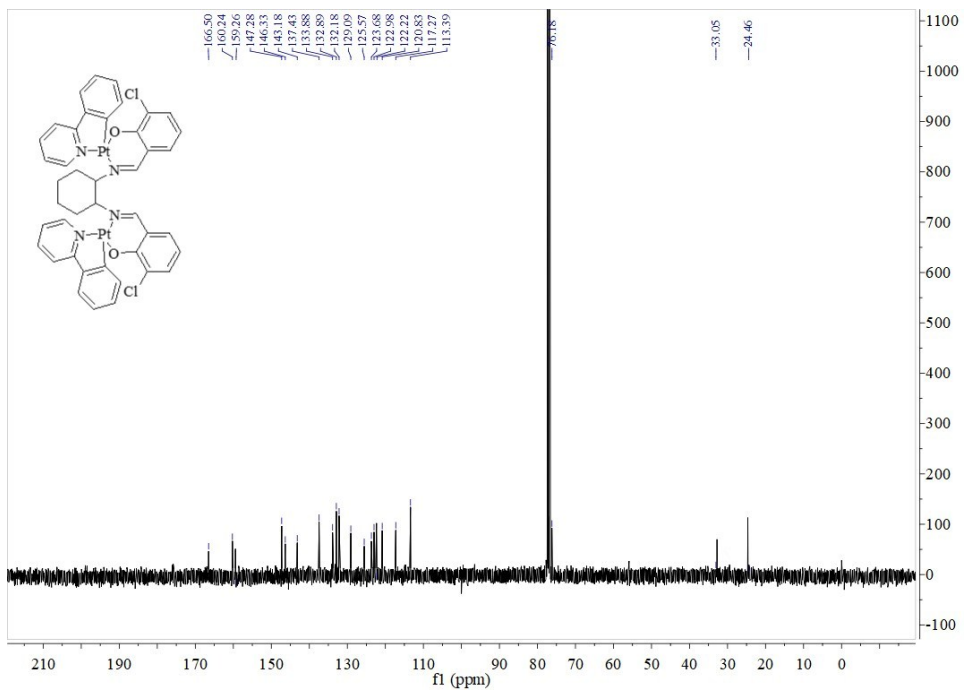
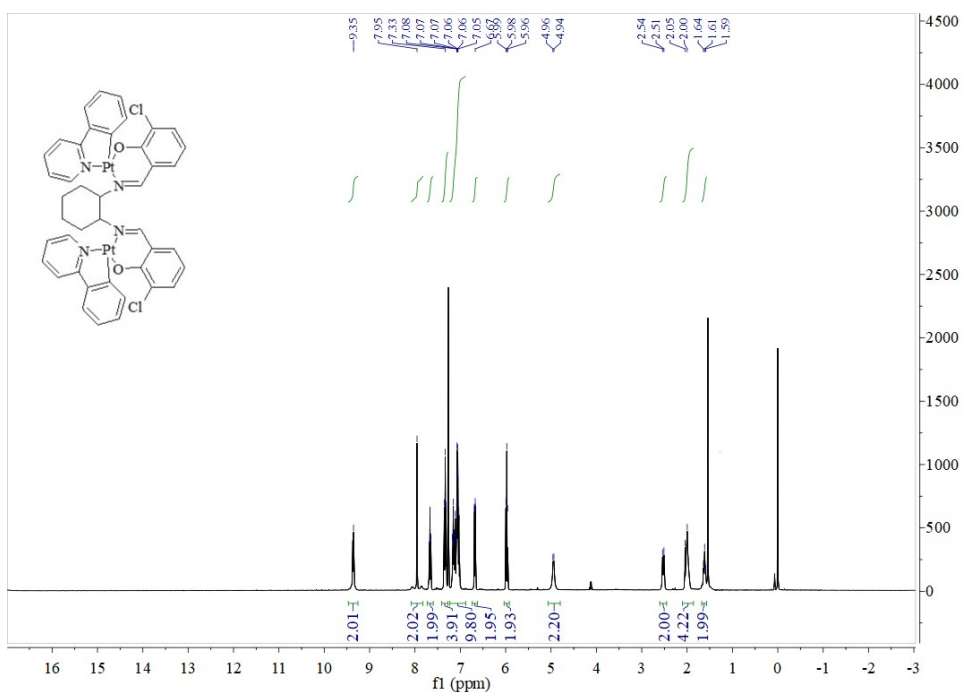
**Fig. S19.** Emission spectra of **ppy-Pt-3-F-(S,S)Cy** in THF/H<sub>2</sub>O with volume fraction of water ( $2.0 \times 10^{-5}$  mol dm<sup>-3</sup>).



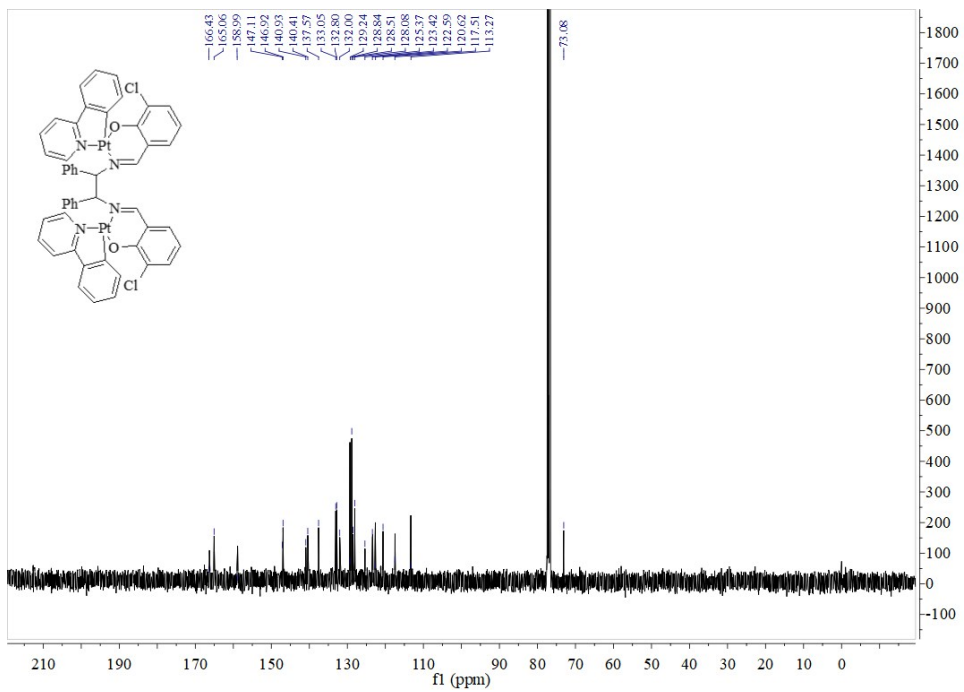
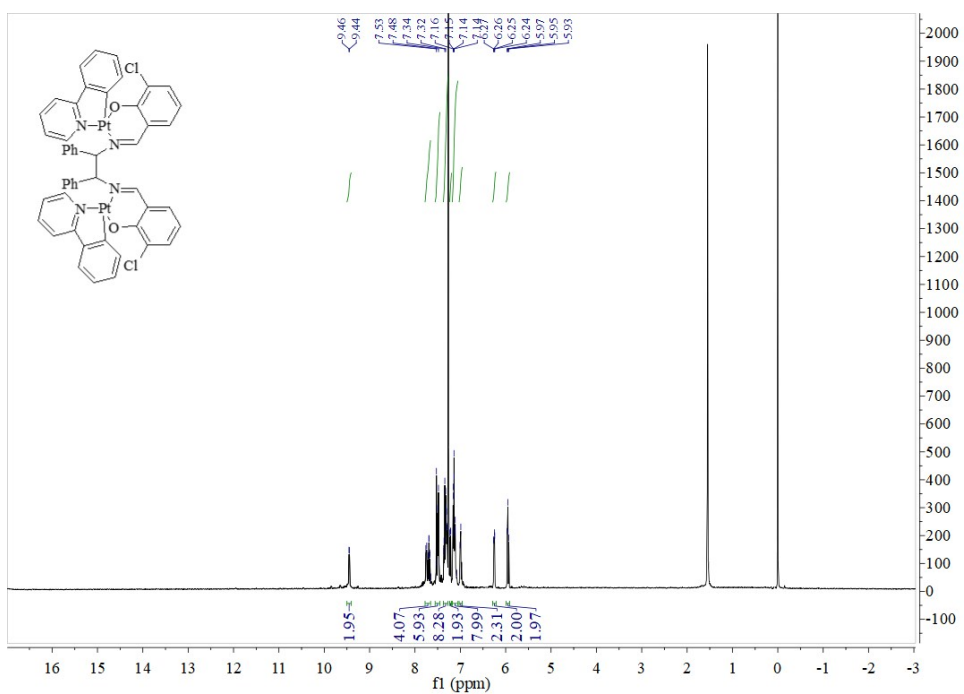
<sup>1</sup>H NMR and <sup>13</sup>C NMR spectra of **ppy-Pt-(R,R)Cy** in CDCl<sub>3</sub>.



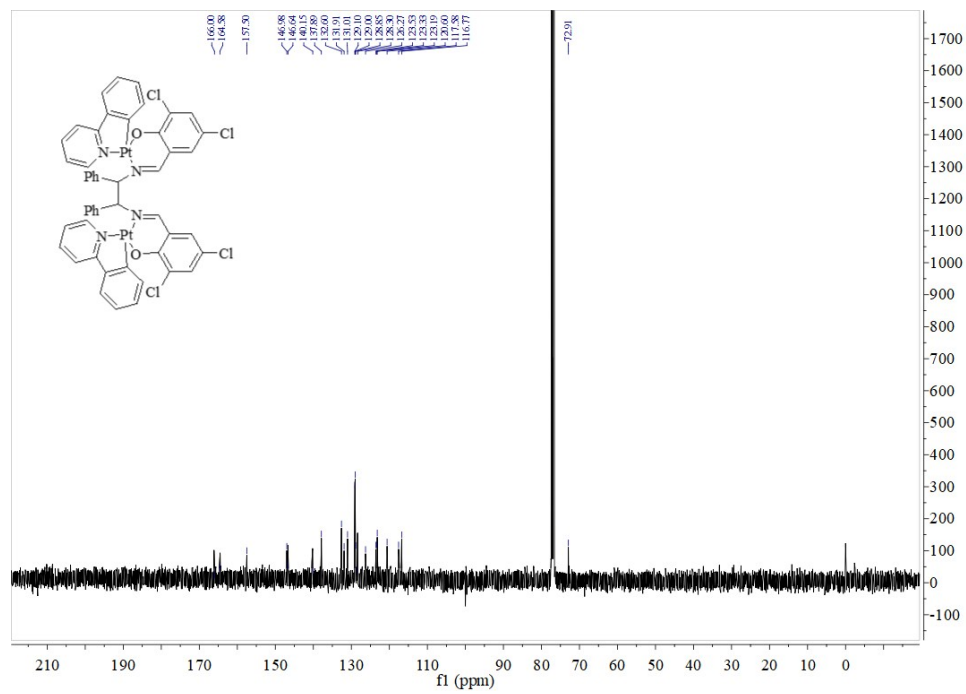
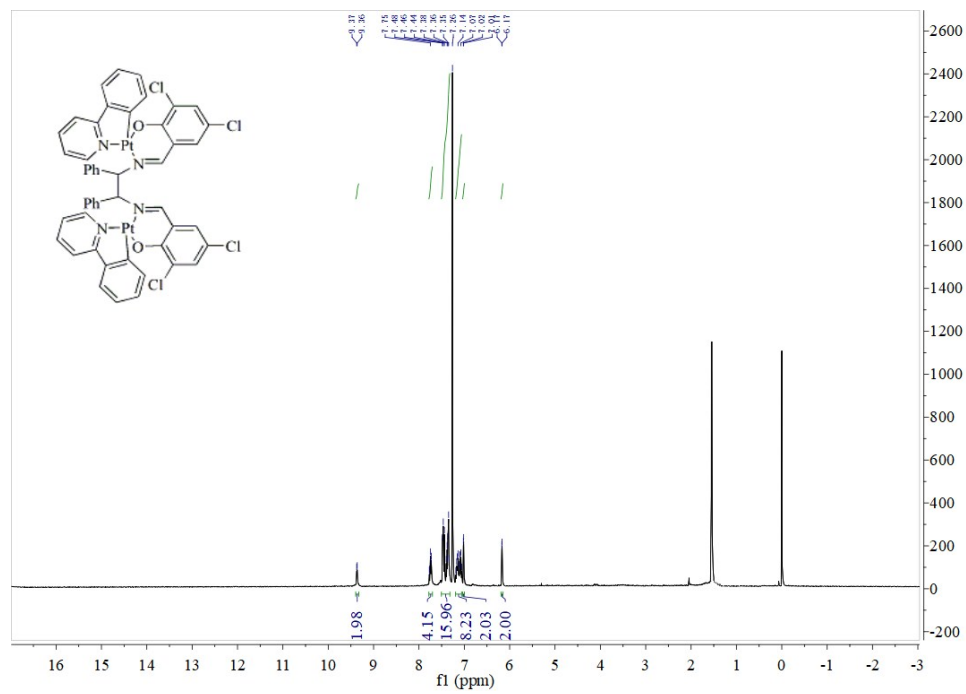
<sup>1</sup>H NMR and <sup>13</sup>C NMR spectra of **ppy-Pt-3-F-(R,R)Cy** in CDCl<sub>3</sub>.



<sup>1</sup>H NMR and <sup>13</sup>C NMR spectra of **ppy-Pt-3-Cl-(R,R)Cy** in CDCl<sub>3</sub>.



$^1\text{H}$  NMR and  $^{13}\text{C}$  NMR spectra of **ppy-Pt-3-Cl-(R,R)diPh** in  $\text{CDCl}_3$ .



<sup>1</sup>H NMR and <sup>13</sup>C NMR spectra of ppy-Pt-3,5-Cl-(R,R)diPh in CDCl<sub>3</sub>.